Pure Appl. Chem., Vol. 85, No. 7, pp. 1389–1403, 2013.
http://dx.doi.org/10.1351/PAC-CON-12-08-16

From elementary reactions to chemical relevance in the photodynamic therapy of cancer*

Luis G. Arnaut[1,2] and Sebastião J. Formosinho[1,‡]

[1]*Chemistry Department, University of Coimbra, 3004-535 Coimbra, Portugal;*
[2]*Luzitin SA, Ed. Bluepharma, S. Martinho do Bispo, 3045-016 Coimbra, Portugal*

Abstract: Theories of radiationless conversions and of chemical processes were employed to design better photosensitizers for photodynamic therapy (PDT). In addition to photostability and intense absorption in the near infrared, these photosensitizers were required to generate high yields of long-lived triplet states that could efficiently transfer their energy, or an electron, to molecular oxygen. The guidance provided by the theories was combined with the ability to synthesize large quantities of pure photosensitizers and with the biological screening of graded hydrophilicities/lipophilicities. The theoretical prediction that halogenated sulfonamide tetraphenylbacteriochlorins could satisfy all the criteria for ideal PDT photosensitizers was verified experimentally.

Keywords: kinetics; oxygen; photochemistry; porphyrins.

INTRODUCTION

This report describes the basic research carried out in our group to develop better photosensitizers for the photodynamic therapy (PDT) of cancer. For a wider perspective on the development of photosensitizers currently used in cancer treatments the readers are referred to the reviews by Dougherty and co-workers [1] and by Bonnett [2]. The complexity of finding promising new drug candidates far exceeds the competences of any given research group, and the development of the photosensitizers described here had instrumental contributions from a group of organic synthesis and a group of biological chemistry. However, the logical development of the present story necessarily sacrifices extensive summaries of their achievements that will be duly reported elsewhere. Our fundamental efforts were guided by a framework of theoretical models linking theories of elementary chemical reactions (involving the rupture and formation of bonds) such as hydrogen- and proton-transfer reactions, with theories of processes, such as radiationless electron or energy transfer, which preserve chemical bonding. Notably, we made extensive use of the tunnel-effect theory (TET) applicable to radiationless transitions in large organic molecules [3–6] to maximize the quantum yields of the photosensitizer triplet states (Φ_T) and of the intersecting/interacting-state model (ISM) [7–9] to model the reactivity of the photosensitizer triplet state with molecular oxygen. It will only be possible to evaluate the success of the new photosensitizers after clinical trials. However, it is already possible to assess the relevance of the semi-empirical models mentioned above in the design of a new class of photosensitizers and its translation from basic research to experimental development.

Pure Appl. Chem.* **85, 1257–1513 (2013). A collection of invited papers based on presentations at the XXIV[th] IUPAC Symposium on Photochemistry, Coimbra, Portugal, 15–20 July 2012.
‡Corresponding author

The initial motivation for our research project was the pathway for the approval in the United States of Photofrin® (a mixture of hematoporphyrin derivatives—HpD) for the treatment of esophageal cancer in 1995 and of lung cancer in 1998 [1], and for the approval in the European Union of Foscan (5,10,15,20-tetrakis(*m*-hydroxyphenyl)chlorin—THPC) for head and neck cancer in 2001 [10]. Porphyrin derivatives have been at the forefront of the photosensitizers investigated for PDT because they have an intrinsic affinity for tumors and strong absorptions in the red, near the phototherapeutic window, where light is most penetrating and less harmful to human tissues. The core of a porphyrin is a tetrapyrrole in which the four rings of the pyrrole type are linked together by methine carbon atoms. The most common reduced porphyrins are dihydroporphyrins, and the parent compound of this series is called chlorin. Tetrahydroporphyrins in which the saturated carbon atoms are located at nonfused carbon atoms of two diagonally opposite pyrrole rings are called bacteriochlorins. Scheme 1 illustrates the key features of porphyrin derivatives and the nomenclature used in this work.

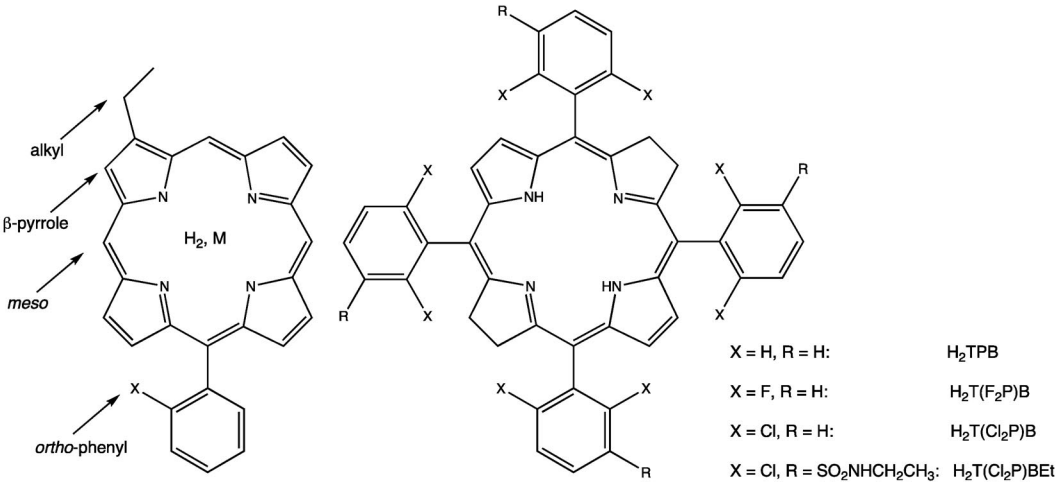

Scheme 1 Porphyrin basic structural elements (left) and acronyms of bacteriochlorins employed in this work (right).

The photosensitizers approved for clinical use in Europe or in the United States have limitations that often relegate them to the fourth treatment option in their therapeutic indications, after surgery, chemotherapy, and radiation therapy. Most noteworthy are the skin photosensitivity 2 to 6 weeks after treatment, the insufficient tissue penetration of the light that activates these photosensitizers, and the long drug-to-light intervals (2 to 5 days). These handicaps can be related to the molecular properties of the photosensitizers and used to define the properties of an ideal photosensitizer for PDT. First we will briefly review the guidelines that have been proposed to design better photosensitizers for PDT and draw the general features of the ideal photosensitizer. Next we will discuss in detail the methods employed to model two critical properties of PDT photosensitizers: the maximization of the triplet quantum yield and the generation of reactive oxygen species (ROS: $^1O_2$, $O_2^{\bullet-}$, H_2O_2, $OH^{\bullet}$). Finally, we will conclude with a possible roadmap for the experimental development of the new photosensitizers.

QUALITATIVE DESIGN CONSIDERATIONS

Guidelines to design better photosensitizers for PDT of cancer have been proposed by various influential authors. Dolphin defined a profile for an ideal PDT drug including strong absorption in the red (>650 nm), high triplet (Φ_T) and $^1O_2$ (Φ_Δ) quantum yields, low dark toxicity, selectivity towards tumor

tissue, simple formulation and long shelf-life, rapid clearance for the body, facile synthesis and feasible scale-up, and strong proprietary position [11]. Jori went further to quantify the most relevant physicochemical properties of an efficient photodynamic agent: 700 nm < λ_{max} < 800 nm, $\varepsilon_{infrared}$ > 10^5 M^{-1} cm^{-1}, $\Phi_F \geq 0.2$, $\Phi_T \geq 0.7$, triplet lifetime $\tau_T \geq 100$ μs, $\Phi_\Delta > 0.5$, and photodegradation quantum yield $\Phi_{pd} < 10^{-5}$ [12]. Pandey emphasized, in addition to some of the properties mentioned before, the requirements of low skin photosensitivity, amphiphilicity (i.e., water-soluble but containing a hydrophobic matrix, to facilitate the crossing of cell membranes), and chemical purity [13]. Although these guidelines were not available in the literature at the beginning of our research program in 1994, they were present in our design of photosensitizers for PDT, as it will be seen below.

The quest for a strong absorption in the phototherapeutic window (700–800 nm) directed our interest to bacteriochlorins. However, it was known that bacteriochlorins were labile and this had led other researchers [2,11] to focus their work on chlorins, which absorb at ca. 650 nm. Indeed, about 25 to 33 % of 5,10,15,20-tetrakis(*m*-hydroxyphenyl)bacteriochlorin (THPB) within cells is oxidized to chlorin in 24 h [14], and its photodecomposition quantum yield is $\Phi_{pd} = 1.5 \times 10^{-3}$ [15,16]. In order to approach the ideal properties of PDT sensitizers, it would be necessary to increase the stability of bacteriochlorins.

Photosensitizers with high $^1O_2$ quantum yields must have long-lived triplet states formed with near-unit quantum yields, and triplet-state energies at least 15 kJ/mol above that of singlet oxygen (E_Δ = 94 kJ/mol). The lifetimes and energies of the triplet states of the bacteriochlorins known at the beginning of our research project met these kinetic and energetic requirements, but the $^1O_2$ quantum yields were modest, $\Phi_\Delta = 0.43$ for THPB in methanol [17]. More importantly, photosensitizers bearing the tetrapyrrole macrocycle have a terrible tendency to aggregate in aqueous solutions and lose most of their ability to generate singlet oxygen. For example, HpD monomer units have $\Phi_\Delta = 0.64$ in methanol but in water HpD is mostly present in the form of dimers with $\Phi_\Delta = 0.11$ [18]. On the other hand, it was also known that steric interactions between *ortho*-substituents on the *meso*-phenyl rings of porphyrins with their H atoms in β-pyrrole positions increases the angle between phenyl rings and the macrocycle, thus preventing the dimerization and aggregation of the porphyrins [19].

Ortho-substituents in tetraphenylporphyrins (TPPs) can also exert other important functions. Selecting substituents with high atomic numbers, it is possible to have an internal heavy atom effect that increases the intersystem crossing rate and, consequently, Φ_T and Φ_Δ. If such substituents are electron-withdrawing groups, they increase the oxidation potential of the photosensitizers, stabilize them against oxidation, and, therefore, decrease Φ_{pd}. Additionally, bulky substituents at the *ortho*-positions can be a source of hindrance against molecular oxygen attack and further stabilize the photosensitizer [20].

These properties of *ortho*-substituted tetraphenylbacteriochlorins were compatible with another determinant of ideal PDT photosensitizers: the economical synthesis from easily accessible precursors. Indeed, Gonsalves and Pereira had perfected a method to prepare TPPs in large quantities and with high purity that met with considerable success in the synthesis of a wide range of such porphyrins [21]. Methods to prepare chlorin and bacteriochlorin derivatives of TPPs have been published elsewhere in collaboration with Pereira [16], and will not be further discussed here. Thus, *ortho*-substituted tetraphenylbacteriochlorins could be synthesized substantially pure and in large quantities and could be tested as templates for improved PDT photosensitizers. These molecular templates had to be decorated with substituents that could facilitate drug administration and yield favorable pharmacokinetics.

Hydrophilic photosensitizers, usually bearing sulfonic or carboxylic acid substituents, are most appealing because they can be administered in aqueous solutions. An overview of the maximal tumor uptake and tumor/peritumoral tissue ratios revealed that photosensitizers with sulfonyl groups tended to perform better than those with carboxylic groups [22]. On the other hand, the diversity of delivery vehicles, animal models, and administration protocols made it very difficult to predict the performance of hydrophilic vs. amphiphilic photosensitizers. For example, the logarithm of the *n*-octanol:water partition coefficient (P_{OW}) of hematoporphyrin IX is 0, whereas that of Foscan is 5.5 [23]. Thus, the biological screening of *ortho*-substituted tetraphenylbacteriochlorins with sulfonyl groups should cover

molecules with log P_{OW} ranging from –2 (e.g., sulfonic acids) to +5 (e.g., sulfonamides with *n*-alkyl groups).

The diffusion distance of singlet oxygen in a cell is ca. 550 nm, much smaller than the 10–30 μm diameter of typical eukaryotic cells [24]. Hence, the space probed by singlet oxygen is a small fraction of the cell volume and the intracellular localization of the photosensitizer is important to determine the initial targets of PDT. Most porphyrins and their derivatives localize at the level of the cell membranes, including cytoplasmic, mitochondrial, and lysosomal membranes, of the Golgi apparatus and of the endoplasmic reticulum (ER) [12,25,26]. A curious exception is *meso*-tetra(4-*N*-methylpyridyl)porphine, a cationic porphyrin, which has been found to localize at the nuclear level in cultured cells [27]. Hydrophilic and anionic photosensitizers are primarily localized in lysosomes. A classic example is 5,10,15,20-tetrakis(4-sulfonatophenyl)porphyrin (TPPS) [28–30]. More lipophilic photosensitizers tend to distribute between the membranes of cellular organelles. After prolonged incubation with A431 cells, Photofrin enters mainly the ER/Golgi apparatus and to a less extent can be found at other perinuclear sites [31,32]. It is also very well established that Foscan® after 3 h of incubation with MCF-7 cells can be found both in the ER and in the Golgi apparatus, but after 24 h it extrudes from the Golgi and is essentially in the ER, with only a weak distribution in the mitochondria [33]. Clearly, the most popular photosensitizers for the PDT take advantage from their localization in the ER to trigger various cell death mechanisms. To some extent, the intracellular localizations of porphyrin derivatives depend on their P_{OW}. This and the tumor uptake are difficult to predict, and therefore the final steps of the selection of the best photosensitizer eventually require in vitro and in vivo screening. The screening of selected drug candidates in appropriate formulations remains a labor-intensive task whose success owes much to the insight and skill of the researchers. This work will not address that step of the development of our photosensitizers, which has been reported in collaboration with Dabrowski [34].

The number of publications per year on "photodynamic therapy" increased by more than a factor of 5 over the last 20 years, but Photofrin and Foscan remain the only photosensitizers widely accepted for the treatment of non-skin cancers in the United States or in the European Union. The apparent implication of this reality is that photosensitizers meeting all the criteria for the ideal PDT drug have not yet been developed. When we first formulated our research program in 1994 [35], we specifically proposed to make an *ortho*-substituted sulfonamide TPP derivative with an absorption extending up to 760 nm, with the expectation that it would meet the criteria for the ideal PDT drug, and specified chlorine atoms as promising *ortho*-substituents. The PDT efficacy of 5,10,15,20-tetrakis(2,6-dichloro-3-*N*-ethylsulfamoylphenyl)bacteriochlorin, $H_2T(Cl_2P)B$, against S91 melanoma tumors implanted in dilute, brown, and non-agouti (DBA) mice [36], shows that the rational for the development of this photosensitizer was correct. In the following sections, we will address in detail the theoretical design of the photochemical properties of our family of photosensitizers and the mechanisms of ROS generation.

OPTIMIZATION OF THE PHOTOSENSITIZER TRIPLET STATE

The spectroscopy of porphyrin and metalloporphyrin derivatives was recently reviewed by one of us, and the reader is referred to that work for the details on their electronic absorption spectra and relation to molecular and electronic structure [37]. Here our first concern is the fate of the singlet state of such photosensitizers. Considering the guidelines discussed above, it would be desirable that most of the singlet states should intersystem cross to the triplet states and a small fraction of them should fluoresce.

We investigated the use of an internal heavy-atom effect in the sensitizer to accelerate the intersystem-crossings $S_1 \rightarrow T_1$ and maximize Φ_T. However, the same effect may also accelerate the intersystem-crossings $T_1 \rightarrow S_0$ and reduce τ_T below 100 μs. Only a judicious choice of internal heavy-atom effects could increase Φ_T without compromising τ_T.

Scheme 1 illustrates several substitution possibilities encompassing also a metal (Me) coordination in the central position of the carbon skeleton ring. In the earlier steps of this research program we have carried out a systematic study of such effects, which were rationalized through the use of a model

for radiationless transitions in large molecules, the TET. Intersystem-crossing rates are a function of the spin–orbit coupling factor, ξ, of an atom with a high atomic number, Z, that outweighs all the other atoms ($\xi \approx Z^4$). Additionally, just like other radiationless transitions in the weak-coupling limit, intersystem-crossing rates present an inverse relationship with the difference in energy, ΔE_{S-T}, of the singlet and triplet states and are also proportional to the relative number of vibrational modes, η, involved in the transition. Under the Wentzel–Kramers–Brillouin (WKB) approximation, TET expresses the tunneling rate as [3]

$$k_{TET} = \chi \nu \exp\left[-\frac{1}{\hbar}\sqrt{2\mu\left(D - E_v\right)}\frac{\Delta x}{\eta}\right] \tag{1}$$

where χ is the electronic factor, ν is the frequency of the vibrational mode, ν_{CH} = 3000 cm^{-1} and ν_{CC} = 1050 cm^{-1}, μ its reduced mass (μ_{CH} = 0.923 and μ_{CC} = 6), D–E_v is the barrier height, Δx the barrier width defined in Fig. 1, and η the relative number of the promoting vibrational modes (i.e., the CH and CC stretching modes). Siebrand [38] has shown empirically that η can be substituted by the relative number of atoms, $\eta_H = n_H/(n_H + n_C + n_X)$ and $\eta_C = n_C/(n_H + n_C + n_X)$, where the number of atoms is represented by: hydrogen (n_H), carbon (n_C), and other atoms (n_X).

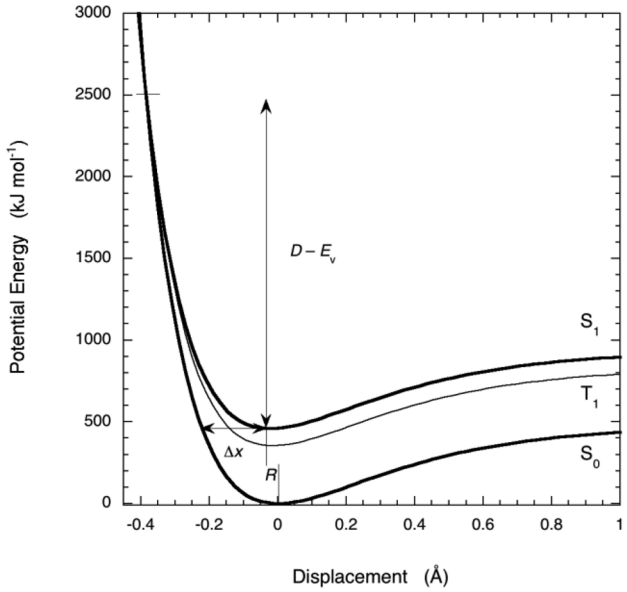

Fig. 1 Schematic barriers for radiationless transitions in large molecules.

The exponential part of the equation represents the Franck–Condon factor between a vibrational wavefunction in the nonadiabatic region of the initial electronic state and a vibrational function in the final state, taken as a δ function at the classical turning points of vibration. Within the context of a golden-rule approach, Jortner and Ulstrup have shown that the Franck–Condon vibrational overlap factors of some radiationless transitions acquires a form practically identical with eq. 1 of TET [39].

The calculation of the Franck–Condon factors requires the knowledge of the nuclear displacement between the initial and final electronic states, and a function to describe the dependence of the energy on the nuclear coordinates. McCoy and Ross [40] showed that the electronic transitions in polycyclic aromatic hydrocarbons can be expressed in terms of a bond-length displacement coordinate R

$$R = \left(\sum_j \Delta r_j^2 \right)^{1/2} \tag{2}$$

where Δr_j represents the change in length of the *j*th bond. In benzene each CH bond contracts by 0.009 Å upon electronic excitation from the S_0 to the S_1 state. This contraction of the CH bonds directs tunneling to the repulsive side of the potential energy curves. A simple way to describe the dependence of the energy on the nuclear coordinates is to employ Morse curves, but the radiationless transitions involve all the promoting modes of a certain type, CH or CC. The role played by CH stretching vibrations in radiationless transitions of aromatic hydrocarbons is better described in terms of local rather than normal modes. A treatment of local modes as independent oscillators leads to the construction of generalized potential-energy curves with generalized Morse parameters, $\beta(CH)=\sqrt[4]{n_H}\ \beta_{CH}$ and $\beta(CC)=\sqrt[4]{n_C}\ \beta_{CC}$.

The description of spin–orbit coupling requires additional parameters, as many as the number of chemically different sites where heavy atoms are introduced. For the simple case of *i* identical heavy atoms in equivalent positions, the nonadiabatic factor can be written as

$$\chi = \chi_0 \left[1 + c(i\xi)^2 \right] \tag{3}$$

where χ_0 is the nonadiabatic factor in the absence of significant spin–orbit coupling, and the coefficient *c* measures the contribution of the *i* identical heavy atoms to the total intersystem-crossing rate. After verifying the success of eqs. 1–3 in the description of $S_2 \rightarrow S_1$, $S_1 \rightarrow S_0$, $S_1 \rightarrow T_1$, and $T_1 \rightarrow S_0$ radiationless transitions for polyaromatic molecules covering a range of ca. 14 orders of magnitude in rates and ca. 425 kJ mol^{-1} in energy gaps, TET was applied to the study of the $S_1 \rightarrow T_1$ and $T_1 \rightarrow S_0$ processes in metallated TPPs, including some with halogens in the phenyl rings, and halogenated porphyrins. The issue was to assess the dependence of the spin–orbit coupling on the substitution pattern of porphyrin derivatives.

The parameter *c* was obtained empirically from the study of a large number of porphyrin derivatives (Scheme 1). Table 1 presents the values of *c* different substitution positions. As inferred from Table 1, heavy atoms in alkyl positions of octaalkylporphyrins (OAPs) are more efficient in accelerating the decay of the triplet state than in promoting its formation. Hence, such porphyrin derivatives are not expected to have long-lived triplet state formed in high yields. On the other hand, a central coordination metal (Me) or halogens in the *ortho*-positions of the phenyl rings of TPP derivatives may give high yields of triplet without compromising triplet lifetimes. The choice of the metal is limited to diamagnetic complexes, because the paramagnetic complexes exhibit low-energy charge-transfer (CT) states that very efficiently quench the excited states [37]. Thus, avoiding toxic metals, the choice is practically limited to Mg, Zn, In, or Pd complexes. Moreover, the introduction of Mg or Zn in the macrocycle leads to lower oxidation potentials and, consequently, lowers the stability of the photosensitizer.

Table 1 Empirical values of the contribution *c* to spin–orbit coupling of heavy atoms in different positions of porphyrin derivatives[a].

Substitution positions	$S_1 \rightarrow T_1$		$T_1 \rightarrow S_0$	
	χ_0	*c*	χ_0	*c*
Alkyl-pyrrole in OAPs	10^{-2}	2×10^{-5}	5×10^{-3}	5×10^{-4}
Alkyl-*meso* in OAPs	10^{-2}	1×10^{-4}	5×10^{-3}	1×10^{-3}
Metal in TPPs	10^{-2}	2×10^{-4}	5×10^{-3}	2×10^{-5}
Ortho-phenyl in TPPs	10^{-2}	2×10^{-6}	5×10^{-3}	5×10^{-7}

[a]OAPs = octaalkylporphyrins, TPPs = tetraphenylporphyrins.

It is instructive to apply eq. 3 to the more promising photosensitizer templates based on the TPP core and predict the effects of the heavy atoms in Φ_T and in τ_T using the literature spin–orbit coupling constants [41]. Free-base H_2TPP is a good starting point because it is known to have τ_S = 12.6 ns, Φ_F = 0.10, Φ_T = 0.73 and a very long triplet lifetime [42–44]. The literature value of τ_T at 300 K in deaerated toluene is τ_T = 1380 μs [45]. In the simulations presented in Table 2 we use the triplet lifetime of H_2TPP to predict the values of Φ_T and τ_T for other photosensitizers assuming that the Franck–Condon factors are not affected by metal or halogen atom substitutions.

Table 2 Prediction of spin–orbit coupling effects on photophysical properties of porphyrin derivatives.

	$i\,\xi$	τ_S/ns	Φ_F	Φ_T	τ_T/μs
H_2TPP	1	12.6	0.10	0.73	1380
In-TPP	1183	0.061	0.0005	0.999	48
Pd-TPP	1504	0.038	0.0003	0.999	30
H_2T(FP)P	4 × 269	4.68	0.0372	0.900	874
H_2T(F_2P)P	8 × 269	1.62	0.0129	0.965	416
H_2T(Cl_2P)P	8 × 587	0.380	0.0030	0.992	115
H_2T(BrP)P	4 × 2460	0.089	0.0007	0.998	28

Table 2 shows that In and Pd complexes should be virtually nonfluorescent and their triplet quantum yields should approach unity. On the other hand, their triplet lifetimes are expected to be relatively short. A very similar pattern is also expected for TPP derivatives with one bromine atom in an *ortho*-position of each phenyl ring. These patterns are manifested in photosensitizers designed for PDT. For example, In-bacteriochlorins have $\tau_S \approx 0.27$ ns, $\Phi_F \approx 0.0018$, and $\tau_T \approx 30$ μs [46]. Pd-bacteriopheophorbide (trade name Tookad), currently in phase III clinical trials for prostate cancer, has τ_S = 0.11 ns and $\tau_T \approx 20$ μs in acetone [47].

Our work on free-base tetraphenylbacteriochlorins with fluorine or chlorine atoms in the *ortho*-position of the phenyl rings revealed that the presence of one F atom in each phenyl ring leads to τ_S = 3.6 ns, Φ_F = 0.13, whereas that of two Cl atoms leads to $\tau_S \approx 0.47$ ns, Φ_F = 0.013, and τ_T = 38 μs [43,44]. This triplet lifetime may be limited by residual oxygen in our N_2-saturated toluene solutions. Again, the spin–orbit coupling of the heavy atoms anticipated the trends observed, even though the changes in Franck–Condon factors were neglected.

The properties of the ideal photosensitizer established above included $\Phi_F \geq 0.2$ and $\Phi_T \geq 0.7$. The maximization of Φ_T is necessarily associated with a decrease in Φ_F. It is very useful to have fluorescence for diagnostic applications and for visualizing the photosensitizer in the optimization of protocols, but it is probably also acceptable to trade diagnostic applications for the ability to maximize the production of ROS. Thus, compounds with $\Phi_F \geq 0.001$ and $\Phi_T \geq 0.95$ are probably the best tradeoff for PDT, leaving some fluorescence for guidance in the use of the photosensitizer.

The ideal photosensitizers should also have $\tau_T \geq 100$ μs to allow for the efficient formation of ROS even in hypoxic tissues. The relevance of this factor is not duly appreciated in solutions of organic solvents at room temperature that have oxygen concentrations in the millimolar range and triplet quenching by oxygen has rate constants $k_q \approx 2 \times 10^9$ M^{-1} s^{-1}. In these conditions, a triplet lifetime of 3 μs is sufficient to have more than 90 % quenching by oxygen. Even in water at 25 °C the concentration of oxygen is still 0.27 mM [41] and 90 % quenching by oxygen only requires τ_T = 17 μs with $k_q \approx 2 \times 10^9$ M^{-1} s^{-1}. However, the diffusion coefficient of oxygen decreases from $D_{O2} = 2 \times 10^{-5}$ cm^2/s in water to 4×10^{-6} cm^2/s in the cells because of the higher viscosity inside the cells [24], and the value of k_q is expected to drop to $k_q \approx 4 \times 10^8$ M^{-1} s^{-1}. Experimental estimates are in the range of (0.8–5.5) × 10^8 M^{-1} s^{-1} [48]. Additionally, the concentration of oxygen in tissues can be much lower than in solution. The value of $[O_2]$ in tissues can be obtained from the partial pressure of oxygen (pO_2) in such tis-

sues and its solubility. A common solubility constant of O_2 employed in tissue solubility is 1.35 μM/mm Hg (10.1 μM/kPa) [49], which is also the solubility of oxygen in pure water at 37 °C. The mean pO_2 value decreases monotonically in the tissue as the distance from the closest blood vessel increases. It was reported that pO_2 decreases from 14 mm Hg in the blood vessel to 5 mm Hg some 70–80 μm away from the closest blood vessel, a value that is taken as the onset of hypoxia [50]. Thus, it is not unlikely that some regions of a tumor have oxygen concentrations below 10 μM. In such regions, 80 % of triplet quenching by oxygen requires τ_T = 1 ms, which is unrealistic. The targeted τ_T = 100 μs should give Φ_Δ = 0.29, and a photosensitizer with τ_T = 10 μs has Φ_Δ = 0.04 at the limit of tumor hypoxia. Thus, in tissues, short triplet lifetimes may limit the success of PDT.

In summary, tetraphenylbacteriochlorin derivatives decorated with fluorine or chlorine atom in an *ortho*-position of each phenyl ring combine $\varepsilon_{infrared} > 10^5$ M^{-1} cm^{-1}, $\Phi_T \geq 0.7$ and $\tau_T \geq 100$ μs with measurable fluorescence, and should be a good template to design ideal photosensitizers for PDT.

OPTIMIZATION OF ROS GENERATION

Long-lived triplet states formed with a near-unit quantum yield and energies above 110 kJ/mol are a prerequisite for the irreversible and efficient formation of singlet oxygen. However, the interaction between the photosensitizer triplet state and molecular oxygen offers various reactive and nonreactive channels that can interfere with the nature of the ROS formed and with their quantum yields of formation. This interaction was elegantly described by Wilkinson [51–53], and a simplified version of the Wilkinson mechanism is presented in Fig. 2, which explicitly consider the formation of superoxide ion, $O_2^{\bullet-}$, in addition to singlet oxygen, $O_2(^1\Delta_g)$ [43]. The salient feature of this mechanism is the competition between CT and non-CT processes [54].

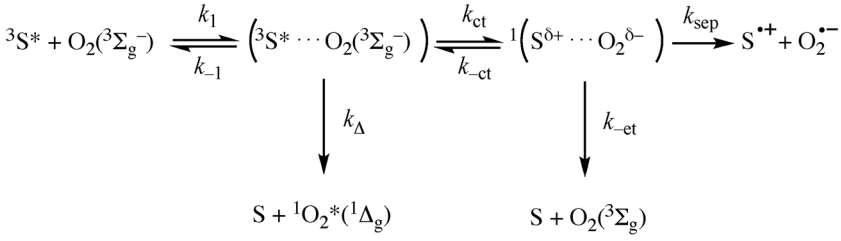

Fig. 2 Simplified Wilkinson mechanism for the quenching of the sensitizer T_1 state (^3S) by O_2 in its ground state $3\Sigma_g^-$.

According to the Wilkinson mechanism, the presence of CT can accelerate the rate of triplet quenching by oxygen but, paradoxically, this will reduce the singlet oxygen quantum yield. As the oxidation potential of the photosensitizer decreases and the CT process becomes more competitive against the non-CT process, k_q increases and Φ_Δ decreases. In the absence of CT, the statistics of spin multiplicities implies that the triplet state is quenched by oxygen with a rate $k_q = (1/9)k_{diff}$, where k_{diff} is the rate of diffusion. In such a case, the oxygen is generated in its singlet state $O_2(^1\Delta_g)$ with a unit yield (Φ_Δ = 1). However, if CT is involved, the quenching rate is higher, $k_q = (4/9)k_{diff}$, but the yield of $^1\Delta_g$ formation decreases to Φ_Δ = 0.25, since there are two channels of reaction: the non-CT channel that generates $O_2(^1\Delta_g)$ and the CT channel that leads back to the ground state of O_2 or to radical ions. According to Table 3, this competition seems to be more relevant in the quenching of bacteriochlorin triplet states than in the quenching of the corresponding porphyrin triplets because the bacteriochlorin quenching rate constants exceed $(1/9)k_{diff}$, estimated as $k_{diff} = 9.5 \times 10^9$ M^{-1} s^{-1} from the quenching of the singlet state of $H_2T(FP)P$ in ethanol.

Table 3 Oxidation potentials and triplet-state properties of TPP and tetraphenylbacteriochlorin derivatives.

	E_D^{ox} V vs. SCE	E_T kJ mol^{-1}	k_q 10^9 M^{-1} s^{-1}	Φ_Δ	k_Δ 10^9 M^{-1} s^{-1}	k_{CT} 10^9 M^{-1} s^{-1}
$H_2T(Cl_2P)PEt$[a]	>1.23	138	0.66	0.85	0.60	0.10
$H_2T(Cl_2P)P$[b]	≈1.23		0.86	0.98	0.93	0.02
$H_2T(F_2P)P$[b]	≈1.23		1.1	0.84	1.2	0.01
H_2TPP[c,d,e]	0.95	138	1.4	0.71	1.6	0.04
$H_2T(Cl_2P)BEt$[a]	>0.68	108	1.8	0.66	1.4	0.76
$H_2T(Cl_2P)B$[d]	≈0.68		2.1	0.60	1.6	1.1
$H_2T(F_2P)B$[d]	≈0.68	103	2.6	0.48	2.0	1.6
H_2TPB	0.40					

[a]Ref. [43].
[b]Ref. [55].
[c]Ref. [56].
[d]Ref. [57].
[e]Ref. [37].

Ogilby and co-workers have also addressed the interaction between aromatic molecules and oxygen, namely, under conditions where a ground-state CT complex can be formed between the dye and oxygen, ($S^{\delta+}\cdots O_2^{\delta-}$) [58]. It was argued that the CT state formed by direct excitation of the ground-state CT complex can also lead to the formation of singlet oxygen, but the value of Φ_Δ was lower in polar solvents where more CT complex is present. This study suggests that a direct pathway from $^1(S^{\delta+}\cdots O_2^{\delta-})$ to S + $^1O_2$ may exist but it is not the dominant decay channel of the excited-state CT complex.

These studies illustrate the relevance of understanding the interaction between the T_1 state of the photosensitizer and oxygen (i.e., the mechanisms of energy and charge transfer) for a proper optimization of ROS generation. Energy and electron transfers are exquisitely entangled in these systems, because they share a common role of Franck–Condon factors, and this a fascinating playground for energy- and electron-transfer models.

The oxidation potentials of H_2TPP and H_2TPB have been determined experimentally and in Table 3 are presented vs. SCE after appropriate corrections [37,59,60]. The oxidation potentials of the *ortho*-halogenated derivatives were estimated by additive corrections from the differences observed in the oxidation potentials of $H_2T(X_2P)P$ derivatives [61]. The presence of a sulfonamide group in the meta position of the phenyl group is expected to further increase the oxidation potential, considering its negative Hammett constant σ_p = –0.46 [41]. The decrease in the oxidation potentials in Table 3 is accompanied by an increase in the quenching rate constants and a decrease in the singlet oxygen quantum yields. These are the trends expected for the transition from a mostly non-CT to a mostly CT process in the Wilkinson mechanism.

The relevance of the CT channel in the quenching of bacteriochlorin triplets requires that the energy of the CT complex formed between such photosensitizers and oxygen approaches that of the corresponding encounter complex. In polar solvents the energy of such complexes can be estimated as that of radical-ion pairs using

$$\Delta G_{rip} = \left(E_D^{ox} - E_A^{red}\right) - \frac{e_0^2}{\varepsilon r_{DA}} \quad (4)$$

where the half-wave reduction potential of oxygen is E_A^{red} = –0.78 V vs. SCE in dimethyl sulfoxide (DMSO) [62]. In polar solvents, such as ethanol, the last term is negligible and the energy of the radi-

cal-ion pair $H_2T(F_2P)B^{\bullet+}/O_2^{\bullet-}$ is 141 kJ/mol, whereas that of the $H_2T(F_2P)P^{\bullet+}/O_2^{\bullet-}$ ion pair is 194 kJ/mol. The energy of the CT state involving the bacteriochlorin is closer to its triplet-state energy than in the analogous porphyrin. More experimental information on the triplet energies and oxidation potentials of these photosensitizers will be necessary to make a quantitative assessment of the CT channel, but the available data are entirely consistent with the increased relevance of CT in the quenching of bacteriochlorins.

Further insight into the rate constants of the non-CT channel (k_Δ) and CT channel (k_{CT}) can be obtained correcting for the effect of diffusion

$$k_D = \frac{k_{-\text{diff}} k_T^Q}{k_{-\text{diff}} - k_T^Q} \tag{5}$$

where $k_{-\text{diff}} = k_{\text{diff}}/1$ M [54]. The triplet lifetimes of these photosensitizers are very long, and their energies are below the energy of the first excited triplet state of molecular oxygen. Under these conditions, all the photosensitizer triplet states are quenched by oxygen in ethanol, and we can express the efficiency of the non-CT channel, which exclusively leads to singlet oxygen, as $F_\Delta = \Phi_\Delta/\Phi_T$. Our best estimate of Φ_T for the photosensitizers with fluorine atoms in the *ortho*-positions of the phenyl rings is $\Phi_T \approx 0.85$ and for the analogous compounds with chlorine atoms is $\Phi_T \approx 1$ [56]. These values together with $\Phi_T = 0.73$ for H_2TPP were employed to obtain the rate constants of the non-CT and CT channels using $k_\Delta = F_\Delta\, k_D$ or $k_{CT} = (1 - F_\Delta)\, k_D$.

Table 3 shows that the values of k_Δ tend to follow the energy-gap law, with the fastest rates observed for the lowest energy triplet states, while the values of k_{CT} tend to increase as the oxidation potential of the photosensitizer is lowered. Interestingly, both trends contribute to make the triplet state of $H_2T(F_2P)B$ the most reactive of these species towards oxygen, with non-CT and CT channels having a very similar contribution.

We mentioned earlier that the ideal photosensitizer should also have $\Phi_\Delta > 0.5$. It may be disheartening to realize that some bacteriochlorins may not meet this criterion. However, the larger extent of CT in bacteriochlorins opens the opportunity for the generation of other ROS.

It was established early in the development of PDT that the phototoxicity of sensitizers could be assigned to two types of processes, named Type-I and Type-II [63]. Type-II photoreactions are commonly associated with singlet oxygen production, and their efficiency depends on Φ_Δ. On the other hand, Type-I photoreactions are associated with electron and proton transfers, eventually leading to superoxide ion, hydrogen peroxide, and hydroxyl radical. These ROS, and specially the hydroxyl radical, are very cytotoxic, and their generation could contribute appreciably to PDT efficacy. The expectation of finding such ROS motivated various research groups to employ probes capable of providing evidence for the presence of these reactive species in solution or in cells during a PDT experiment. Electron paramagnetic resonance (EPR) spectra of spin adducts with $O_2^{\bullet-}$, $HOO^\bullet$, or $OH^\bullet$ have been observed with Zn-phthalocyanine [64], protoporphyrins [65], bacteriochlorin *a* [66], Zn-bacteriochlorin [67], Pd-bacteriopheophorbide [47,68], and halogenated tetraphenylbacteriochlorins [43,69]. Additionally, probes that react preferentially with $OH^\bullet$ and become fluorescent have been employed to identify the presence of this species in cells following PDT [70–72]. Although it is certain that these ROS are formed during PDT with some sensitizers, their relevance for PDT efficacy in some cases remains controversial. For example, Hayett and co-workers did not find any correlation between cell kill and superoxide levels generated by protoporphyrins [65], presumably because these levels were too low under their experimental conditions, while Scherz and co-workers claimed that the phototoxicity of a water-soluble derivative of Pd-bacteriopheophorbide (Tookad-soluble) is exclusively due to $O_2^{\bullet-}$ and $OH^\bullet$ radicals [68], with no contribution from singlet oxygen. We found a synergistic phototoxicity effect between $O_2^{\bullet-}$ and $OH^\bullet$ radicals and singlet oxygen [72].

Disparate mechanisms have been proposed for the formation of these ROS in aerated solutions in the absence of electron donors. It was suggested that quenching of the triplet Zn-phthalocyanine [64] or Zn-bacteriochlorin [67] by the ground-state photosensitizer could give a radical-ion pair

$$^3S + S \rightarrow S^{\bullet+} + S^{\bullet-}$$

This is only energetically possible if the triplet energy of the photosensitizer is higher than the highest occupied molecular orbital-lowest unoccupied molecular orbital (HOMO-LUMO) gap measured by E_S^{ox}–E_S^{red}. Although Fukuzumi and co-workers claimed that Zn-bacteriochlorin has E_S^{ox}–E_S^{red} = 122 kJ/mol and E_T = 135 kJ/mol, it is very unlikely that the E_T of this photosensitizer is only 7 kJ/mol below its E_S because the singlet-triplet splitting of tetrapyrroles is typically 40 kJ/mol and the HOMO-LUMO gap is correlated with E_S rather than E_T [37]. Furthermore, such a small singlet-triplet splitting associated with a long triplet lifetime should lead to delayed fluorescence, but the authors reported a single exponential fit to the singlet lifetime of 0.89 ns [67].

Alternatively, for bacteriochlorin *a* [66], Pd-bacteriopheophorbide [47,68], and halogenated tetraphenylbacteriochlorins [43], full electron transfer from the bacteriochlorin to oxygen was proposed

$$^3S + O_2 \rightarrow S^{\bullet+} + O_2^{\bullet-}$$

The energetic restrictions imposed by eq. 4 for this electron-transfer reaction limit its relevance to photosensitizers with low E_S^{ox} and/or high E_T. This electron-transfer step eventually followed by a proton-transfer reaction

$$(H)S^{\bullet+} + O_2^{\bullet-} \rightarrow S^{\bullet} + {}^{\bullet}HO_2$$

where the radical $S^{\bullet}$ is formed from the photosensitizer by donation of a H atom. In the cellular environment there are other possible sources of H atoms, and $S^{\bullet+}$ can be reduced back to the ground-state photosensitizer S.

Another possibility that should be considered is a proton-coupled electron transfer (PCET) [73,74]

$$(H)^3S + O_2 \rightarrow S^{\bullet} + {}^{\bullet}HO_2$$

The photosensitizer was represented in the reactions above as (H)S to emphasize its role as the source of H atoms. The feasibility of this reaction, which is formally a formal H-atom transfer, must also be assessed in terms of its thermodynamics. Thus, the enthalpy of the reaction initiated by the triplet state of the photosensitizer is

$$\Delta H_r = [D_0(S) - D_0({}^{\bullet}HO_2)] - E_T$$

where D_0 represents the H-bond dissociation energies determined at 298 K. Considering that $D_0({}^{\bullet}HO_2)$ = 204 ± 3 kJ/mol [75] and given the values of E_T in Table 3, thermodynamic considerations exclude both the homolytic cleavages of N–H bonds in the sulfonamide [76] or in the pyrrol nitrogen [77] as the sources of the H atoms because they would lead to $\Delta H_r > 50$ kJ/mol. There is an alternative source of H atoms in bacteriochlorin derivatives, which are the H atoms bonded to the saturated carbon atoms located at the nonfused carbon atoms of the reduced pyrrole ring. PCET with the electron coming from the macrocycle and the proton coming from the methylene carbon atoms of the reduced pyrrole rings, or a formal H-abstraction reaction, shown in Scheme 2, have the same thermochemistry and are energetically possible in view of the enthalpies of formation of 1-pyrroline and pyrrole.

Abstraction of the two H atoms in the pyrroline unit by the same oxygen molecule would give hydrogen peroxide while abstraction by two oxygen molecules would give two hydroperoxyl radicals, both with the concomitant oxidation of the bacteriochlorin to the chlorin. This mechanism is consistent with the photo-oxidation of THPB to THPC [78,79] and of Pd-bacteriopheophorbide to chorin and porphyrin derivatives [47], and also with our own observations on the photodecomposition of sulfonated

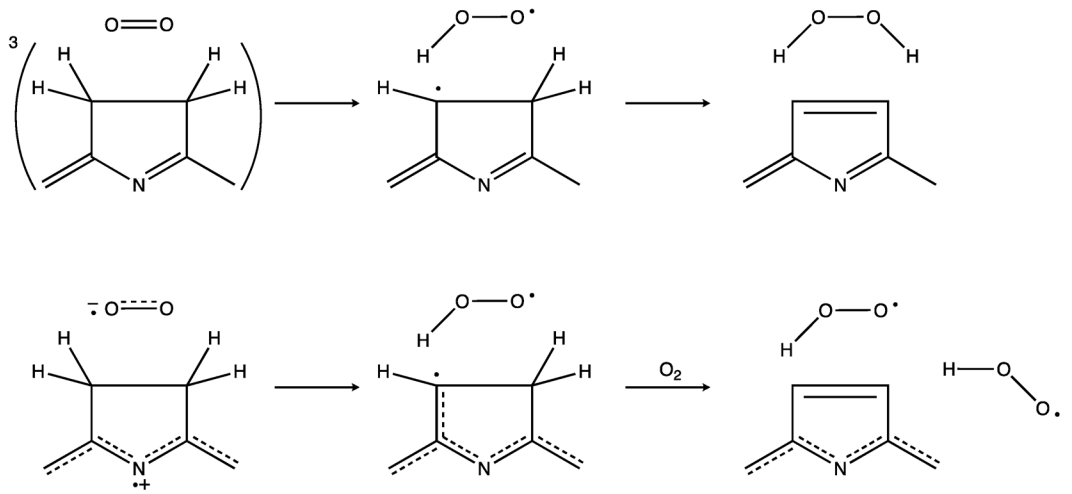

Scheme 2 Mechanisms of PCET leading to the oxidation of a chlorin to a porphyrin (or a bacteriochlorin to a chlorin) with the formation of ROS.

and halogenated tetraphenylbacteriochlorins that yield the corresponding chlorins as one of the products.

The controlled photodecomposition was also identified as a parameter relevant to characterize the ideal properties of a photosensitizer. Electron- or atom-transfer reactions leading to ROS such as $O_2^{\bullet-}$, H_2O_2, and $OH^{\bullet}$ increase the phototoxicity of the sensitizer but may also increase its photodecomposition. For example, THPB has $\Phi_{pd} = 1.5 \times 10^{-3}$ in methanol:water and Tookad has $\Phi_{pd} = 1.8 \times 10^{-3}$ in acetone [16]. This facile photodecomposition is consistent with the low oxidation potentials expected for these bacteriochlorins, in particular with $E_S^{ox} = 0.40$ vs. SCE (0.23 V vs. $FeCp^+/FeCp$ [80]) for Tookad. A contrasting behavior occurs in TPPS, which has $\Phi_{pd} = 9.8 \times 10^{-6}$ in buffer of pH 7 [81], consistent with its $E_S^{ox} = 1.1$ V vs. SCE [82]. The value of $\Phi_{pd} = 6 \times 10^{-6}$ for $H_2T(Cl_2P)BEt$ in PBS:methanol is also consistent with the high E_S^{ox} expected for this photosensitizer, and approaches the properties of an ideal photosensitizer for PDT.

In summary, halogenated sulfonamide tetraphenylbacteriochlorins also meet the criteria of $\Phi_\Delta > 0.5$ and $\Phi_{pd} < 10^{-5}$ for the ideal photosensitizer, with the additional feature that they can also generate very cytotoxic hydroxyl radicals.

CONCLUDING REMARKS

Theoretical models provided the guidance to the development of better sensitizers for PDT, namely, anticipating that sulfonamide tetraphenylbacteriochlorins with Cl or F atoms in the *ortho*-positions of the phenyl groups could meet the photochemical criteria for ideal photosensitizers: $\varepsilon_{infrared} > 10^5$ M^{-1} cm^{-1}, $\Phi_T \geq 0.7$, $\tau_T \geq 100$ μs, $\Phi_\Delta > 0.5$ and $\Phi_{pd} < 10^{-5}$. Furthermore, these compounds have measurable fluorescence, generate $O_2^{\bullet-}$, H_2O_2, and $OH^{\bullet}$, and are amphiphilic with log P_{OW} ca. 2. Although these properties are required for the success of PDT photosensitizers, they are not sufficient. The development of such sensitizers also requires a facile synthesis and feasible scale-up. The synthesis of halogenated sulfonamide bacteriochlorins requires only three steps from widely available materials and is simple to scale-up. Finally, the criteria of simple formulation, selectivity towards tumor tissue, rapid clearance for the body, and low skin photosensitivity, are currently being tested, but the results obtained with DBA mice with implanted S91 melanoma tumors [36] are encouraging.

The pathway to regulatory approval of new drugs is increasingly long and expensive, while the success rate of new drugs tends to decrease. Given this scenario, it is particularly gratifying to see that theoretical models of radiationless transitions and chemical processes can position the starting point of drug development on a faster and more promising track.

ACKNOWLEDGMENTS

The authors are much indebted to Mariette M. Pereira for the invaluable collaboration in the synthesis of porphyrin derivatives since 1996, and to Janusz M. Dabrowski for the talented biological studies with such porphyrin derivatives since 2006. We thank FCT-FEDER (PTDC/QUI-QUI/120182/2010) for financial support.

REFERENCES

1. T. J. Dougherty, C. J. Gomer, B. W. Henderson, G. Jori, D. Kessel, M. Korbelik, J. Moan, Q. Peng. *J. Natl. Cancer Inst.* **90**, 889 (1998).
2. R. Bonnett. *Chem. Soc. Rev.* **24**, 19 (1995).
3. S. J. Formosinho. *J. Chem. Soc., Faraday Trans. 2* **70**, 605 (1974).
4. S. J. Formosinho. *Mol. Photochem.* **7**, 41 (1976).
5. S. J. Formosinho. *J. Chem. Soc., Faraday Trans. 2* **72**, 1313 (1976).
6. S. J. Formosinho, L. G. Arnaut. *Adv. Photochem.* **16**, 67 (1991).
7. S. J. Formosinho, L. G. Arnaut, R. Fausto. *Prog. React. Kinet.* **23**, 1 (1997).
8. L. G. Arnaut, S. J. Formosinho, H. D. Burrows. *Chemical Kinetics*, Elsevier, Amsterdam (2007).
9. L. G. Arnaut, S. J. Formosinho. *Chem.—Eur. J.* **14**, 6578 (2008).
10. Z. Huang. *Technol. Cancer Res. Treat.* **4**, 283 (2005).
11. E. D. Sternberg, D. Dolphin, C. Brucker. *Tetrahedron* **54**, 4151 (1998).
12. G. Jori. In *CRC Handbook of Organic Photochemistry and Photobiology*, F. Lenci, W. Horspool (Eds.), pp. 146–141, CRC Press (2004).
13. M. Ethirajan, C. Saenz, A. Gupta, M. P. Dobhal, R. K. Pandey. In *Advances in Photodynamic Therapy*, M. R. Hamblin, P. Mroz (Eds.), pp. 13–40, Artech House, Norwood, MA (2008).
14. M. F. Grahn, A. McGuinness, R. Benzie, R. Boyle, M. L. de Jode, M. G. Dilkes, B. Abbas, N. S. Williams. *J. Photochem. Photobiol., B* **37**, 261 (1997).
15. R. Bonnett, B. D. Djelal, P. A. Hamilton, G. Martinez, F. Wierrani. *J. Photochem. Photobiol., B* **53**, 136 (1999).
16. M. M. Pereira, C. J. P. Monteiro, A. V. C. Simões, A. M. A. Pinto, A. R. Abreu, G. F. F. Sá, E. F. F. Silva, L. B. Rocha, J. M. Dabrowski, S. J. Formosinho, S. Simões, L. G. Arnaut. *Tetrahedron* **66**, 9545 (2010).
17. R. Bonnett, P. Charlesworth, B. D. Djelal, D. J. McGarvey, T. G. Truscott. *J. Chem. Soc., Perkin Trans. 2* 325 (1999).
18. C. Tanielian, C. Schweitzer, R. Mechin, C. Wolff. *Free Radical Biol. Med.* **30**, 208 (2001).
19. T. P. G. Sutter, R. Rahimi, P. Hambright, J. C. Bommer, M. Kumar, P. Neta. *J. Chem. Soc., Faraday Trans.* **89**, 495 (1993).
20. A. M. S. Silva, M. G. P. M. S. Neves, R. R. L. Martins, J. A. S. Cavaleiro, T. Boschi, P. Tagliatesta. *J. Porphyrins Phthalocyanines* **2**, 45 (1998).
21. A. M. d. A. R. Gonsalves, J. M. T. B. Varejão, M. M. Pereira. *J. Heterocycl. Chem.* **28**, 635 (1991).
22. R. W. Boyle, D. Dolphin. *Photochem. Photobiol.* **64**, 469 (1996).
23. B. Cunderlíková, O. Kaalhus, R. Cunderlík, A. Mateásik, J. Moan, M. Kongshaug. *Photochem. Photobiol.* **79**, 242 (2004).
24. P. R. Ogilby. *Photochem. Photobiol. Sci.* **9**, 1543 (2010).

25. A. P. Castano, T. N. Demidowa, M. R. Hamblin. *Photodiag. Photodyn. Ther.* **1**, 279 (2004).
26. H. Mojzisova, S. Bonneau, C. Vever-Bizet, D. Brault. *Biochim. Biophys. Acta: Biomembranes* **1768**, 2748 (2007).
27. M. K. Kuimova, M. Balaz, H. L. Anderson, P. R. Ogilby. *J. Am. Chem. Soc.* **131**, 7948 (2009).
28. K. Berg, A. Western, J. C. Bommer, J. Moan. *Photochem. Photobiol.* **52**, 481 (1990).
29. Z. Malik, I. Amit, C. Rothmann. *Photochem. Photobiol.* **65**, 389 (1997).
30. R. Sailer, W. S. L. Strauss, H. Emmert, K. Stock, R. Steiner, H. Schneckenburger. *Photochem. Photobiol.* **71**, 460 (2000).
31. Y.-J. Hsieh, C.-C. Wu, C.-J. Chang, J.-S. Yu. *J. Cell. Physiol.* **194**, 363 (2003).
32. Y.-J. Hsieh, J.-S. Yu, P.-C. Lyu. *J. Cell. Biochem.* **111**, 821 (2010).
33. S. Marchal, A. François, D. Dumas, F. Guillemin, L. Bezdetnaya. *Br. J. Cancer* **96**, 944 (2007).
34. J. M. Dabrowski, L. G. Arnaut, M. M. Pereira, C. J. P. Monteiro, K. Urbanska, S. Simões, G. Stochel. *ChemMedChem* **5**, 1770 (2010).
35. S. J. Formosinho. In *Projectos Aprovados em Concursos antes de 1999*. Fundação para a Ciência e a Tecnologia, Lisbon (1994). http://www.fct.mctes.pt//projectos/proj98/index.html
36. J. M. Dabrowski, L. G. Arnaut, M. M. Pereira, K. Urbanska, G. Stochel. *Med. Chem. Commun.* **3**, 502 (2012).
37. L. G. Arnaut. *Adv. Inorg. Chem.* **63**, 187 (2011).
38. W. Siebrand. In *The Triplet State*, A. B. Zahlan et al. (Eds.), p. 31, Cambridge University Press (1967).
39. J. Jortner, J. Ulstrup. *Chem. Phys. Lett.* **63**, 236 (1979).
40. E. F. McCoy, I. G. Ross. *Aust. J. Chem.* **15**, 573 (1962).
41. M. Montalti, A. Credi, L. Prodi, M. T. Gandolfi. *Handbook of Photochemistry*, Taylor & Francis, Boca Raton, FL (2006).
42. M. Pineiro, A. L. Carvalho, M. M. Pereira, A. M. d. A. R. Gonsalves, L. G. Arnaut, S. J. Formosinho. *Chem.—Eur. J.* **4**, 2299–2307 (1998).
43. E. F. F. Silva, C. Serpa, J. M. Dabrowski, C. J. P. Monteiro, L. G. Arnaut, S. J. Formosinho, G. Stochel, K. Urbanska, S. Simoes, M. M. Pereira. *Chem.—Eur. J.* **16**, 9273 (2010).
44. C. J. P. Monteiro, J. Pina, M. M. Pereira, L. G. Arnaut. *Photochem. Photobiol. Sci.* **11**, 1233 (2012).
45. J. R. Darwent, P. Douglas, A. Harriman, G. Porter, M.-C. Richoux. *Coord. Chem. Rev.* **44**, 83 (1982).
46. M. Krayer, E. Yang, H.-J. Kim, H. L. Kee, R. M. Deans, C. E. Sluder, J. R. Diers, C. Kirmaier, D. F. Bocian, D. Holten, J. S. Lindsey. *Inorg. Chem.* **50**, 4607 (2011).
47. Y. Vakrat-Haglili, L. Weiner, V. Brumfeld, A. Brandis, Y. Salomon, B. McIlroy, B. C. Wilson, A. Pawlak, M. Rozanowska, T. Sarna, A. Scherz. *J. Am. Chem. Soc.* **127**, 6487 (2005).
48. P. A. Firey, T. W. Jones, G. Jori, M. A. J. Rodgers. *Photochem. Photobiol.* **48**, 357 (1988).
49. R. Springett, H. M. Swartz. *Antioxid. Redox Signal.* **9**, 1295 (2007).
50. G. Helmlinger, F. Yuan, M. Dellian, R. K. Jain. *Nat. Med.* **3**, 177 (1997).
51. F. Wilkinson. *Pure Appl. Chem.* **69**, 851 (1997).
52. F. Wilkinson, A. A. Abdel-Shafi. *J. Phys. Chem. A* **101**, 5509 (1997).
53. A. Abdel-Shafi, F. Wilkinson. *J. Phys. Chem. A* **104**, 5747 (2000).
54. R. Schmidt, F. Shafii, C. Schweitzer, A. Abdel-Shafi, F. Wilkinson. *J. Phys. Chem. A* **105**, 1811 (2001).
55. M. Pineiro, M. M. Pereira, A. M. d. A. R. Gonsalves, L. G. Arnaut, S. J. Formosinho. *J. Photochem. Photobiol., A* **138**, 147 (2001).
56. M. Pineiro, A. M. d. A. R. Gonsalves, M. M. Pereira, S. J. Formosinho, L. G. Arnaut. *J. Phys. Chem. A* **106**, 3787 (2002).
57. M. Pineiro. Ph.D. Dissertation, University of Coimbra, Coimbra (Portugal) (2001).

58. P.-G. Jensen, J. Arnbjerg, L. P. Tolbod, R. Toftegaard, P. R. Ogilby. *J. Phys. Chem. A* **113**, 9965 (2009).
59. C. K. Chang, L. K. Hanson, P. F. Richardson, R. Young, J. Fajer. *Proc. Natl. Acad. Sci. USA* **78**, 2652 (1981).
60. J. Fajer, D. C. Borg, A. Forman, R. H. Felton, D. Dolphin, L. Vegh. *Proc. Natl. Acad. Sci. USA* **71**, 994 (1974).
61. Y.-J. Tu, H. C. Cheng, I. Chao, C.-R. Cho, R.-J. Cheng, Y. O. Su. *J. Phys. Chem. A* **116**, 1632 (2012).
62. C. Huang, M. Tian, Y. Yang, F. Guo, M. Wang. *J. Electroanal. Chem.* **272**, 179 (1989).
63. I. J. MacDonald, T. J. Dougherty. *J. Porphyrins Phthalocyanines* **5**, 105 (2001).
64. C. Hadjur, G. Wagnières, F. Ihringer, P. Monnier, H. van der Bergh. *J. Photochem. Photobiol., B* **38**, 196 (1997).
65. A. K. Haylett, F. I. McNair, D. McGarvey, N. J. F. Dodd, E. Forbes, T. G. Truscott, J. V. Moore. *Cancer Lett.* **112**, 233 (1997).
66. M. Hoebeke, H. J. Schuitmaker, L. E. Jannink, T. M. A. R. Dubbelman, A. Jakobs, A. van de Vorst. *Photochem. Photobiol.* **66**, 502 (1997).
67. S. Fukuzumi, K. Ohkubo, X. Zheng, Y. Chen, R. K. Pandey, R. Zhan, K. M. Kadish. *J. Phys. Chem. B* **112**, 2738 (2008).
68. I. Ashur, R. Goldschmidt, I. Pinkas, Y. Salomon, G. Szewczyk, T. Sarna, A. Scherz. *J. Phys. Chem. A* **113**, 8027 (2009).
69. J. M. Dabrowski, K. Urbanska, L. G. Arnaut, M. M. Pereira, A. R. Abreu, S. Simões, G. Stochel. *ChemMedChem* **6**, 465 (2011).
70. M. Price, J. J. Reiners, A. M. Santiago, D. Kessel. *Photochem. Photobiol.* **85**, 1177 (2009).
71. P. Mroz, Y.-Y. Huang, A. Szokalska, T. Zhiyentayev, S. Janjua, A.-P. Nifli, M. E. Sherwood, C. Ruzié, K. E. Borbas, D. Fan, M. Krayer, T. Balasubramanian, E. Yang, H. L. Kee, C. Kirmaier, J. R. Diers, D. F. Bocian, D. Holten, J. S. Lindsey, M. R. Hamblin. *FASEB J.* **24**, 3160 (2010).
72. J. M. Dabrowski, L. G. Arnaut, M. M. Pereira, K. Urbanska, S. Simões, G. Stochel, L. Cortes. *Free Radical Biol. Med.* **52**, 1188 (2012).
73. M. Barroso, L. G. Arnaut, S. J. Formosinho. *J. Phys. Org. Chem.* **21**, 659 (2008).
74. L. G. Arnaut. In *Proton-Coupled Electron Transfer: A Carrefour of Chemical Reactivity Traditions*, S. J. Formosinho, M. Barroso (Eds.), pp. 32–56, Royal Society of Chemistry, Cambridge (2012).
75. M. Litorja, B. Ruscic. *J. Electron Spectrosc. Relat. Phenom.* **97**, 131 (1998).
76. F. G. Bordwell, J. A. Harrelson Jr., T.-Y. Lynch. *J. Org. Chem.* **55**, 3337 (1990).
77. L. G. Arnaut, S. J. Formosinho, M. Barroso. *J. Mol. Struct.* **786**, 207 (2006).
78. H.-P. Lassalle, L. Bezdetnaya, V. Iani, A. Juzeniene, F. Guillemin, J. Moan. *Photochem. Photobiol. Sci.* **3**, 999 (2004).
79. H.-P. Lassalle, N. Lourette, B. Maunit, J.-F. Muller, F. Guillemin, L. Bezdetnaya-Bolotine. *J. Mass Spectrom.* **40**, 1149 (2005).
80. D. Noy, L. Fiedor, G. Hartwich, H. Scheer, A. Scherz. *J. Am. Chem. Soc.* **120**, 3684 (1998).
81. R. Bonnett, G. Martínez. *Tetrahedron* **57**, 9513 (2001).
82. K. Kalyanasundaram, M. Neumann-Spallart. *J. Phys. Chem.* **86**, 5163 (1982).

